Optical properties of superconducting $Bi_2Sr_2CaCu_2O_8$

J. Kobayashi, T. Asahi, M. Sakurai, M. Takahashi, and K. Okubo

Kagami Memorial Laboratory for Materials Science and Technology, Waseda University, 2-8-26, Nishi-Waseda, Shinjuku-ku,
Tokyo 169, Japan

Y. Enomoto

Superconductivity Research Laboratory, International Superconductivity Technology Center, 1-10-13, Shinonome, Koto-ku,
Tokyo 135, Japan

A fundamental optical study was performed on superconducting $Bi_2Sr_2CaCu_2O_8$ by using a high-accuracy universal polarimeter (HAUP). As this crystal is strongly linearly dichroic, we developed the extended HAUP theory which includes the treatments of the optical dichroisms. After having determined the optical nature of the crystal, we applied the extended HAUP method to a thin (001) plate specimen with light traveling to the front and rear directions in the specimen. These two experiments permitted us to separate the reciprocal and nonreciprocal optical effects. No sign of the nonreciprocal effects was found in the HAUP transmission experiment. A gyration tensor component g_{33} takes place suddenly at T_c (90 K), increases with decreasing temperature, and reaches 1.87×10^{-4} (36°/mm of rotatory power) at 15 K. A steep change of birefringence Δn with temperature also occurs below T_c. From the behaviors of g_{33} and Δn with temperature, it can be concluded that the crystal undergoes a second-order phase transition at T_c into an optically active class. The crystal manifests large linear dichroism, i.e., $\Delta m = -2.2 \times 10^{-2}$.

I. INTRODUCTION

One of the most interesting proposals of the theory of high-temperature superconductors (HTSC's) is ''anyon'' superconductivity by Laughlin.[1] He insisted that in two-dimensional space there exist specific particles known as anyons. These particles manifest superconductivity when they are electrically charged. A striking characteristic of such a superconductor is that in its ground state parity and time-reversal symmetries are violated.[2] It then follows that if a HTSC is truly an anyon superconductor, light which has transmitted, should show nonreciprocal rotation of polarization equivalent to the Faraday effect.[2,3] On the other hand, if light is reflected from the HTSC, it is expected to produce the polar Kerr effect.[2,3] Therefore the examination of such optical effects in superconducting materials has been an urgent problem. However, from the experimental point of view, detection of both effects is extremely difficult primarily since they are concealed by the overwhelmingly large birefringence of the specimens.

Lyons *et al.*[4] found the presence of the polar Kerr effect in $YBa_2Cu_3O_{7-x}$ (YBCO) films at a temperature much higher (250 K) than T_c by detecting changes of the rotation angle of circular dichroism (CD). They also found the same effect in the cubic bismuthate superconductor[5] $Ba_{1-x}Rb_xBiO_3$, where the two-dimensional nature of the electrons was lost. This fact was puzzling from the viewpoint of the anyon theory, but Lyons *et al.* suggested that some other mechanisms for the CD phenomenon should be sought for bismuthate superconductors. They[6] improved the apparatus to be only sensitive to nonreciprocal effects, and observed the same effect in YBCO films on the $SrTiO_3$ substrate, but failed to see the effect in films on $LaAlO_3$. Interestingly the nonreciprocal signals disappeared this time

from another bismuthate $Ba_{1-x}K_xBiO_3$. They attributed the reasons for the negative results on YBCO to the small sizes of domains and bismuthates to sample inhomogeneity.

Spielman and co-workers[7–9] developed a Sagnac interferometer which is exclusively sensitive to nonreciprocal effects. They performed both transmission and reflection experiments on $Bi_2Sr_2CaCu_2O_8$ (BSCCO) single crystals and YBCO thin films. They found no signals corresponding to the nonreciprocal effect. It is to be noticed that their method could not be applied to the detection of any reciprocal effects. Weber *et al.*[10] measured optical gyration of BSCCO single crystals by transmission and CD of YBCO single crystals by reflection. They found a surprisingly large gyration, ~2800°/mm in rotatory power, which appeared in BSCCO below 140 K.

According to our experiences of measuring optical activity (OA) of various kinds of solids,[11] we were concerned that the previous authors did not seem to pay sufficient attention to the systematic errors of the various optical devices used in their experimental systems, e.g., $\lambda/4$ plates, Faraday cells, etc. We knew that even the insertion of glass plates or lenses in the light beam compromises seriously the accuracy of the measurements of OA. It seems to us therefore that one is not ready to draw any conclusions on optical phenomena which reflect symmetry breaking of parity and time reversal in HTSC's. Rather fundamental optical properties of HTSC's have not been properly measured. For instance, birefringences and domain texture of any HTSC's have not been clarified at this time. These facts motivated us to begin systematic optical studies on any of the HTSC's drawing as much cautions to eliminating systematic errors as possible.

We developed the high-accuracy universal polarimeter (HAUP),[12–14] which enables one to measure simultaneously OA, birefringence, and the rotation angles of the indicatrix of

crystals with any symmetries. In the HAUP measurements the specimens are placed in the vacuum, and no solid materials are inserted in the light beam passing through the polarizer-specimen-analyzer (P-S-A) system. Therefore any systematic errors except those relating to the polarizer and analyzer are perfectly excluded. In addition, systematic errors due to parasitic ellipticities p and q (Ref. 12) of the polarizer and analyzer, and the small error angle δY (Ref. 13) occurring in setting up the crossed Nicols can be eliminated reasonably in the HAUP method. Therefore searches for optical properties of HTSC's are appropriate to our HAUP method. However HTSC's are almost opaque to visible light. Therefore it is very likely that there exists nonnegligible linear dichroism (LD) in these crystals. The original HAUP theory[12] does not contain any treatment of dichroisms. Therefore we must first extend the HAUP method to be applicable to the crystals with any dichroisms. This paper reports optical properties of one of the HTSC's, BSCCO, revealed by the extended HAUP method where large LD is present.

II. EXTENDED HAUP METHOD

A. Principle

Moxon and Renshaw,[15] and Dijkstra, Meekes, and Kremers[16] have attempted to extend the original HAUP to include dichroisms. They used Jones matrices[17] directly including dichroisms, and derived approximate formulas of intensities of light emerging from the P-S-A system with extremely small dichroisms. In deriving these formulas they duly allowed for the characteristic features of p and q. Dijkstra, Meekes, and Kremers[16] represented the results in the characteristic two-dimensional (θ', Y') coordinates after having introduced the apparent extinction angle θ_0,[12] where θ' and Y' designate the apparent azimuth angle and deflection angle from the crossed Nicols position.[12,13] Moxon and Renshaw[15] did not represent their formulas in these coordinates since they did not include the influence of δY. The presence of δY has already been shown by our various measurements of OA of solids.[13,18,19] Dijkstra, Meekes, and

Kremers[16] did not apply their formulas to any measurements of dichroisms. Moxon, Renshaw, and Tebbutt[20] reported measurements of dichroisms of $NiSO_4 \cdot 6H_2O$ by their method.[15] However, the descriptions of the processes of deriving its dichroisms were too small to check them in detail. In the present case we needed the extended HAUP theory, which is applicable to crystals with considerable dichroism. For this purpose it was necessary to derive afresh the general equations of the extended HAUP. Following that, we applied the approximation conditions to them for being properly applicable to our problem.

We define the N matrix[17] of the extended HAUP method as Θ_H. It consists of four N matrices as follows:

$$\Theta_H = \Theta_3 + \Theta_4 + \Theta_5 + \Theta_6 = \begin{bmatrix} ig_0 + p_0 & -(\omega + i\delta) \\ \omega + i\delta & -(ig_0 + p_0) \end{bmatrix}, \tag{1}$$

where the numbers of the subscripts of Θ refer to Jones' original paper,[17] and

$$\omega = \frac{1}{2}\left(\frac{2\pi}{\lambda}\right)(n_l - n_r) \equiv \frac{\pi}{\lambda}\frac{G}{\bar{n}}, \tag{2}$$

$$g_0 = \frac{1}{2}\left(\frac{2\pi}{\lambda}\right)(n_y - n_x) \equiv \frac{1}{2}\frac{1}{d}\Delta, \tag{3}$$

$$\delta = \frac{1}{2}\left(\frac{2\pi}{\lambda}\right)(m_r - m_l) \equiv \frac{1}{2}\frac{1}{d}\kappa, \tag{4}$$

and

$$p_0 = \frac{1}{2}\left(\frac{2\pi}{\lambda}\right)(m_y - m_x) \equiv \frac{1}{2}\frac{1}{d}E. \tag{5}$$

Here ω, g_0, δ, and p_0 designate circular birefringence, linear birefringence, CD, and LD; n and m refractive index and absorption coefficient; r and l right-handed and left-handed circularly polarized light; and $\bar{n}$ and d mean refractive index and thickness of the specimen. Then the Jones matrix $\mathbf{M}_H$ of the extended HAUP can be readily derived as

$$\mathbf{M}_H = \begin{bmatrix} \cosh Qd + (ig_0 + p_0)\dfrac{\sinh Qd}{Q} & -(\omega + i\delta)\dfrac{\sinh Qd}{Q} \\ (\omega + i\delta)\dfrac{\sinh Qd}{Q} & \cosh Qd - (ig_0 + p_0)\dfrac{\sinh Qd}{Q} \end{bmatrix}, \tag{6}$$

where

$$Q = \sqrt{(p_0 + ig_0)^2 - (\omega + i\delta)^2} \equiv x + iy. \tag{7}$$

The Jones vectors $\mathbf{P}$ and $\mathbf{A}$ of the polarizer and analyzer are expressed as

$$\mathbf{P} = \begin{bmatrix} \cos\theta \cos p + i \sin\theta \sin p \\ \sin\theta \cos p - i \cos\theta \sin p \end{bmatrix}, \tag{8}$$

and

$$\mathbf{A} = \begin{bmatrix} -\sin(\theta + Y)\cos q + i \cos(\theta + Y)\sin q \\ \cos(\theta + Y)\cos q + i \sin(\theta + Y)\sin q \end{bmatrix}, \tag{9}$$

where θ represents azimuth angle of the polarizer, Y is the deflecting angle of the analyzer from the crossed Nicols position. Then the relative intensity ratio of the transmitted light from the P-S-A system is given as[16]

$$I/I_0 = |\mathbf{A}^\dagger \mathbf{M}_H \mathbf{P}|^2, \tag{10}$$

where I and I_0 represent the intensities of the emergent light from the optical system and of the incident light, respectively. Here HAUP conditions[12] are applied; say, $p \approx 10^{-3}$ (rad), $q \approx 10^{-3}$ (rad), $\theta \ll 1.7 \times 10^{-2}$ (rad), and $Y \ll 1.7 \times 10^{-2}$ (rad). These four quantities will be retained in the equations up to second powers. In this case, the relative intensity is expressed

$$I/I_0 = A(\theta) + B(\theta)Y + CY^2, \tag{11}$$

where

$$A(\theta) = H_{11} + H_{12}\theta + H_{13}\theta^2,$$

$$B(\theta) = H_{21} + H_{22}\theta,$$

and

$$C = H_{31}.$$

Each coefficient H_{ij} was calculated. The results are collected in the Appendix.

(11) can be represented in the (θ, Y') coordinate system by considering the systematic error δY of Y,[13]

$$I/I_0 = A'(\theta) + B'(\theta)Y' + C'Y'^2, \tag{12}$$

where

$$A'(\theta) = H'_{11} + H'_{12}\theta + H'_{13}\theta^2,$$

$$B'(\theta) = H'_{21} + H'_{22}\theta,$$

and

$$C' = H'_{31}.$$

Each coefficient H'_{ij} is expressed by the previous ones,

$$H'_{11} = H_{11} + \delta Y H_{21} + \delta Y^2 H_{31}, \tag{13}$$

$$H'_{12} = H_{12} + \delta Y H_{22},$$

$$H'_{13} = H_{13},$$

$$H'_{21} = H_{21} + 2\delta Y H_{31},$$

$$H'_{22} = H_{22},$$

and

$$H'_{31} = H_{31}.$$

Here θ_0 can be obtained by solving the condition that $(\partial/\partial\theta)(I/I_0)_{Y'=0} = 0$,[12]

$$\theta_0 = -\frac{H'_{12}}{2H'_{13}} = -\frac{(p+q)\{(g_0 x - p_0 y)\sinh 2xd + (p_0 x + g_0 y)\sin 2yd\}}{2(p_0^2 + g_0^2)(\cosh 2xd - \cos 2yd)}$$

$$-\frac{\delta Y\{(p_0 x + g_0 y)\sinh 2xd + (p_0 y - g_0 x)\sin 2yd\}}{2(p_0^2 + g_0^2)(\cosh 2xd - \cos 2yd)} - \frac{1}{2}\delta Y + \frac{p_0\omega + g_0\delta}{2(p_0^2 + g_0^2)}. \tag{14}$$

Then it becomes possible to introduce the θ' coordinate by referring to θ_0. The coefficient H''_{ij} in the (θ', Y') coordinate system are expressed

$$I/I_0 = A''(\theta') + B''(\theta')Y' + C''Y'^2, \tag{15}$$

$$A''(\theta') = H''_{11} + H''_{12}\theta' + H''_{13}\theta'^2,$$

$$B''(\theta') = H''_{21} + H''_{22}\theta',$$

and

$$C'' = H''_{31}.$$

Each coefficient is expressed as follows:

$$H''_{11}: \text{ a term independent of } \theta' \text{ and } Y', \tag{16}$$

$$H''_{12} = H'_{12} + 2\theta_0 H'_{13} = 0, \tag{17}$$

$$H''_{13} = H'_{13} = \frac{2(p_0^2 + g_0^2)(\cosh 2xd - \cos 2yd)}{x^2 + y^2}, \tag{18}$$

$$H''_{21}=H'_{21}+\theta_0 H'_{22}=\frac{(p_0\delta-g_0\omega)(g_0 x-p_0 y)\sinh 2xd}{(x^2+y^2)(p_0^2+g_0^2)}+\frac{(p_0\delta-g_0\omega)(p_0 x+g_0 y)\sin 2yd}{(x^2+y^2)(p_0^2+g_0^2)}$$

$$+\frac{(p-q)\{(g_0 x-p_0 y)\sinh 2xd+(p_0 x+g_0 y)\sin 2yd\}}{x^2+y^2}$$

$$-\frac{(p+q)\{(p_0 x+g_0 y)^2-(p_0 y-g_0 x)^2\}\sinh 2xd\ \sin 2yd}{(x^2+y^2)(p_0^2+g_0^2)(\cosh 2xd-\cos 2yd)}$$

$$+\frac{(p+q)(p_0 x+g_0 y)(p_0 y-g_0 x)(\sinh^2 2xd-\sin^2 2yd)}{(x^2+y^2)(p_0^2+g_0^2)(\cosh 2xd-\cos 2yd)}$$

$$+\frac{\delta Y\{(x^2+y^2-\omega^2-\delta^2)\cosh 2xd+(x^2+y^2+\omega^2+\delta^2)\cos 2yd\}}{x^2+y^2}$$

$$-\frac{\delta Y\{(p_0 x+g_0 y)^2\sinh^2 2xd+(p_0 y-g_0 x)^2\sin^2 2yd\}}{(x^2+y^2)(p_0^2+g_0^2)(\cosh 2xd-\cos 2yd)}$$

$$+\frac{2\,\delta Y(p_0 x+g_0 y)(p_0 y-g_0 x)\sinh 2xd\ \sin 2yd}{(x^2+y^2)(p_0^2+g_0^2)(\cosh 2xd-\cos 2yd)},\tag{19}$$

$$H''_{22}=H'_{22}=\frac{2(p_0^2+g_0^2)(\cos 2xd-\cos 2yd)}{x^2+y^2}+\frac{2\{(p_0 x+g_0 y)\sinh 2xd+(p_0 y-g_0 x)\sin 2yd\}}{x^2+y^2},\tag{20}$$

and

$$H''_{31}=H'_{31}=\frac{(p_0^2+g_0^2-\omega^2-\delta^2+x^2+y^2)\cosh 2xd}{2(x^2+y^2)}-\frac{(p_0^2+g_0^2-\omega^2-\delta^2-x^2-y^2)\cos 2yd}{2(x^2+y^2)}$$

$$+\frac{(p_0 x+g_0 y)\sinh 2xd+(p_0 y-g_0 x)\sin 2yd}{x^2+y^2}.\tag{21}$$

Now let us apply the approximation conditions of the present experiment to the above equations. The conditions are as follows; circular birefringence and CD are extremely small compared with linear birefringence and LD, viz.,

$$g_0,p_0\gg\omega>\delta\neq 0,$$

and

$$\omega^2=\delta^2=\omega\delta=0.\tag{22}$$

It must be noted that no conditions are imposed on the magnitude of LD here. If it becomes apparent afterwards that (22) is not appropriate to the present experiments, we will reconsider (22). From (7)

$$x=p_0,\ \ \text{and}\ \ y=g_0.\tag{23}$$

Then H''_{ij} and θ_0 are expressed

$$H''_{13}=e^E+e^{-E}-2\ \cos\Delta,\tag{24}$$

$$H''_{21}=\frac{2\,\delta Y\ \sin^2\Delta}{e^E+e^{-E}-2\ \cos\Delta}$$

$$-\frac{2\ \sin\Delta\{(p-q)\cos\Delta-pe^{-E}+qe^E\}}{e^E+e^{-E}-2\ \cos\Delta}$$

$$+\frac{(p_0\delta-g_0\omega)}{p_0^2+g_0^2}\sin\Delta,\tag{25}$$

$$H''_{22}=2(e^E-\cos\Delta),\tag{26}$$

$$H''_{31}=e^E,\tag{27}$$

and

$$\theta_0=\frac{-(p+q)\sin\Delta}{e^E+e^{-E}-2\ \cos\Delta}-\frac{(e^E-\cos\Delta)\,\delta Y}{e^E+e^{-E}-2\ \cos\Delta}+\frac{(p_0\omega+g_0\delta)}{2(p_0^2+g_0^2)}.\tag{28}$$

The last term in (25) becomes

$$\frac{(p_0\delta-g_0\omega)}{p_0^2+g_0^2}\sin\Delta=\frac{(p_0/g_0)(\delta/g_0)-(\omega/g_0)}{(p_0/g_0)^2+1}\sin\Delta$$

$$=\frac{2\{(E/\Delta)k'-k\}}{(E/\Delta)^2+1}\sin\Delta$$

$$=\frac{2\{Kk'-k\}}{K^2+1}\sin\Delta\doteq\frac{-2k}{K^2+1}\sin\Delta,\tag{29}$$

where

$$k=\frac{\omega}{2g_0},\ \ k'=\frac{\delta}{2g_0},\ \ \text{and}\ \ K=\frac{p_0}{g_0}=\frac{E}{\Delta}.$$

Similarly the last term in (28) becomes

$$\frac{(p_0\omega+g_0\delta)}{2(p_0^2+g_0^2)}=\frac{(E/\Delta)k+k'}{(E/\Delta)^2+1}=\frac{Kk+k'}{K^2+1}.\tag{30}$$

These equations were not derived by Moxon and Renshaw.[15] On the other hand, (25) is not exactly the same as (22) in the paper of Dijkstra, Meekes, and Kremers[16] even if E is small enough to the extent that $e^E\doteq1+E$. It goes without saying that these equations become the original HAUP equations[12] in the case when $p_0=\delta=0$,

$$H''_{13}=4\ \sin^2\frac{\Delta}{2},\tag{31}$$

$$H''_{21}=(p-q-2k)\sin\Delta+2\,\delta Y\ \cos^2\frac{\Delta}{2},\tag{32}$$

$$H''_{22}=4\ \sin^2\frac{\Delta}{2},\tag{33}$$

$$H''_{31}=1,\tag{34}$$

and

$$\theta_0=-\frac{1}{2}(p+q)\cot\frac{\Delta}{2}-\frac{1}{2}\,\delta Y.\tag{35}$$

B. Application to tourmaline (elbaite)

In order to examine the validity of our extended HAUP equations (24)–(28), we tried to measure simultaneously linear birefringence and LD of green tourmaline (elbaite), $NaLi_3Al_6(OH)_4(BO_3)_3Si_6O_{16}$, which is known to have large LD, by using them. As it belongs to optically inactive C_{3v} class,[21,22] the extended HAUP equations become

$$I=I_0A''(\theta')+I_0B''(\theta')Y'+I_0C''Y'^2,\tag{36}$$

$$A''(\theta')=H''_{11}+(e^E+e^{-E}-2\ \cos\Delta)\theta'^2,\tag{37}$$

$$B''(\theta')=\frac{2\,\delta Y\ \sin^2\Delta}{e^E+e^{-E}-2\ \cos\Delta}$$

$$-\frac{2\ \sin\Delta\{(p-q)\cos\Delta-pe^{-E}+qe^E\}}{e^E+e^{-E}-2\ \cos\Delta}$$

$$+2(e^E-\cos\Delta)\theta',\tag{38}$$

$$C''=e^E,\tag{39}$$

and

$$\theta_0=\frac{-(p+q)\sin\Delta}{e^E+e^{-E}-2\ \cos\Delta}-\frac{(e^E-\cos\Delta)\delta Y}{e^E+e^{-E}-2\ \cos\Delta}.\tag{40}$$

A (100) plate specimen with thickness of 1.20 mm was prepared. An Ar laser with wavelength $\lambda=514.5$ nm was used as the light source. θ_0 was determined first at room temperature. Then intensities of transmitted light were determined as double functions of θ' and Y'. Values of $I_0A''(\theta')$, $I_0B''(\theta')$, and I_0C'' at each θ' position were determined by least-squares fittings. I_0C'' values are plotted against θ' in Fig. 1(a), where they were found to be constant irrespective of the change of θ'. Then I_0e^E was obtained from the figure. Figure 1(b) depicts I_0A'' with respect to θ'^2. As a linear relation holds there, $I_0(e^E+e^{-E}-2\ \cos\Delta)$ could be determined from the derivative of the straight line. Furthermore, since I_0B'' was also found to change linearly with respect to θ' as shown in Fig. 1(c), $2I_0(e^E-\cos\Delta)$ and $I_0B''(0)$ were obtained from the derivative and the intercept of the straight line, respectively. Thus I_0, Δ, and e^E could be calculated from I_0e^E, $I_0(e^E+e^{-E}-2\ \cos\Delta)$, and $2I_0(e^E-\cos\Delta)$, and consequently $B''(0)$ from $I_0B''(0)$. Results are as follows: $E=3.4\times10^{-1}$ rad, $\Delta=290$ rad, and $B''(0)=-7.82\times10^{-4}$. Thus p_0 was calculated as

$$p_0=\frac{E}{2d}=1.40\times10^{-4}\ [\mu m^{-1}].\tag{41}$$

Wilkins, Farrell, and Naiman[23] measured wavelength dependences of absorption coefficients m_a and m_c along the a and c axes. p_0 can be estimated from the difference of them as $2.55\times10^{-4}[\mu m^{-1}]$ ($\lambda=500$ nm). The agreement is not perfect. However, considering first that Wilkins, Farrell, and Naiman[23] intended to measure only wavelength dispersions of m_a and m_c separately, and second that the metal concentrations might not be the same in both specimens, the present agreement can be acceptable as having proved the validity of our formulas. The birefringence was calculated as

$$\Delta n=\frac{\lambda}{2\pi d}\Delta=1.97\times10^{-2}.\tag{42}$$

It is in good agreement with the previous report, say, $\Delta n=2.0\times10^{-2}$.[24] Thus we could conclude that our formulas for the extended HAUP method were correct.

III. OPTICAL PROPERTIES OF $Bi_2Sr_2CaCu_2O_8$

A. Optical nature

In order to obtain BSCCO single crystals, a mixture of BiO_2, $SrCO_3$, $CaCO_3$, and CuO_2 in the molar ratios of
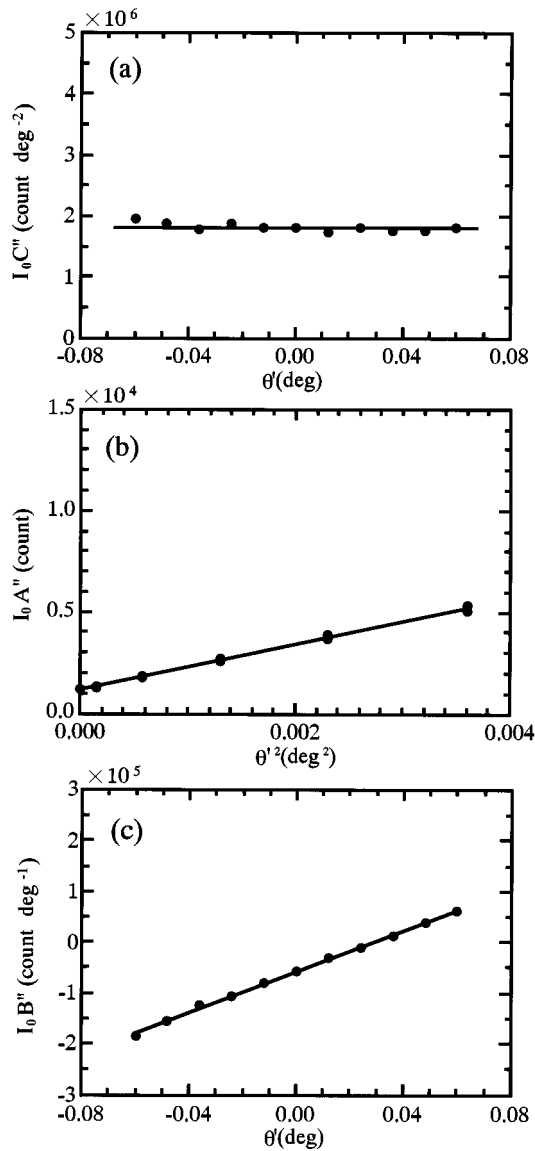
FIG. 1. I_0C'' vs θ' (a), I_0A'' vs θ'^2 (b), and I_0B'' vs θ' (c) for the (100) plate specimen of elbaite at room temperature.

1:2:1:8 was melted in a platinum crucible at 1170 K. A single crystal, $5.5 \times 6.7 \times 2.3$ mm^3 in dimensions, was grown by a slow cooling of the melt. A very thin (001) plate specimen with area of 320×273 μm^2 and thickness of 0.66 ± 0.05 μm could be successfully prepared by making use of the cleaving habit of the crystal along (001) planes. The thickness of the specimen was measured by using a scanning electron microscope. The polarizing microscopic observation unequivocally revealed that the specimen consisted of a single domain. The specimen was also investigated by x rays using the Weissenberg method to confirm the above observation and to measure the lattice constants; $a = 5.43$ Å, $b = 5.44$ Å, $c = 30.96$ Å, which are in good agreement with previous reports.[25]

By using a quartz wedge attached to the polarizing microscope the optical nature in the (001) plane was easily determined as $n_a < n_b$. Then the sequence of the magnitudes of the refractive indices along the principal axes must correspond to any of the following three cases: (i) $n_a < n_b < n_c$, (ii) $n_a < n_c < n_b$, and (iii) $n_c < n_a < n_b$. We tested the specimen by the conoscopic method. Figure 2(a) indicates the conoscopic interference figure in the extinction position. An isogyre parallel to the b axis looked slightly bolder than that parallel to the a axis. Figure 2(b) indicates the figure when the specimen was in the diagonal position. It is clearly seen that the melatopes are located on the a axis and the isogyres are symmetrically disposed with respect to the center of the figure. This fact unambiguously showed that (010) plane is the optical plane and n_b must be the optical Y axis. Thus the correct optical nature was determined to be the case (i). In order to confirm this result, the insertion of a gypsum test plate to the (b) position showed the addition of interference color. The optical nature of BSCCO is represented in Fig. 2(c).

B. HAUP measurements

The extended HAUP equations (24)–(28) were applied to the same BSCCO specimen as used in the optical study. One edge of the specimen was glued to a thin Cu plate with a small opening of a diameter of about 100 μm to pass the light beam. The HAUP measurements were performed twice on this specimen; the first measurements with light passing
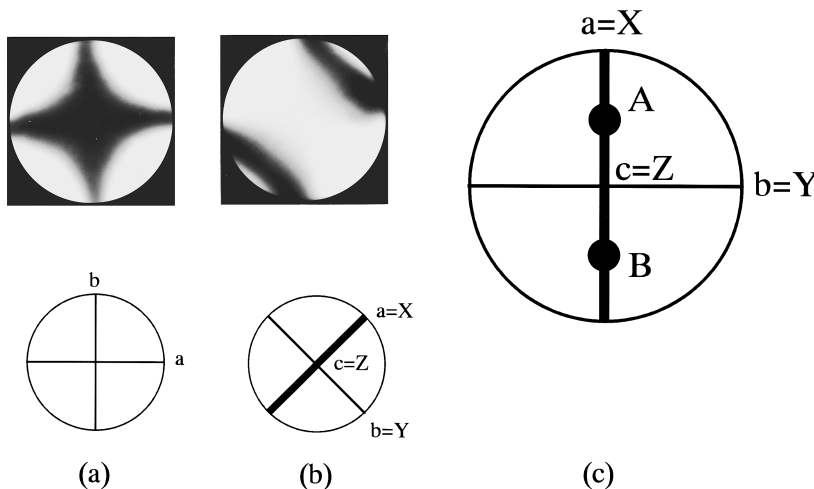
FIG. 2. Conoscopic figures of BSCCO, (a) in the extinction position, and (b) in the diagonal position. (c) represents optical orientation of BSCCO, A and B denoting the optic axes.

J. KOBAYASHI *et al.*
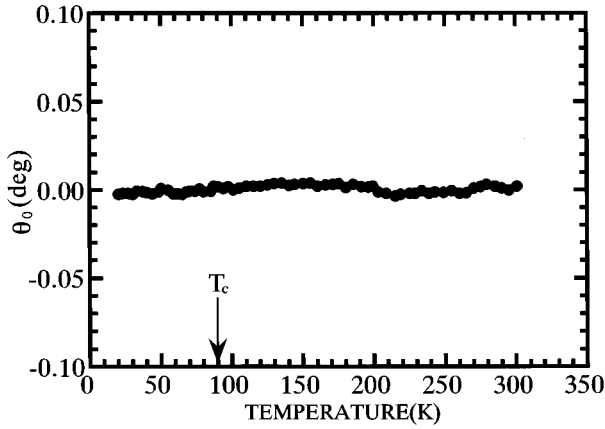
FIG. 3. Temperature dependence of extinction position θ_0 of BSCCO.
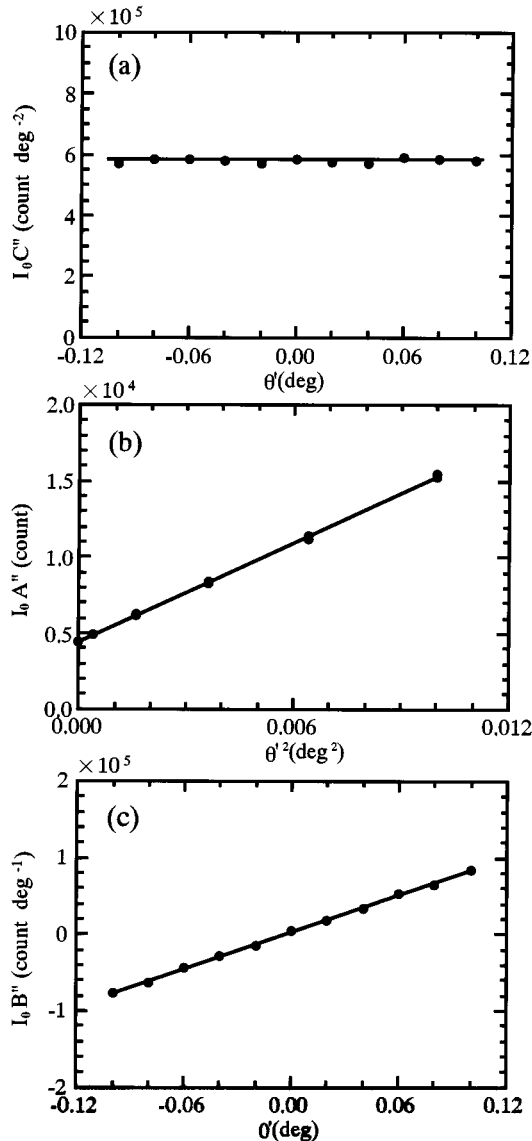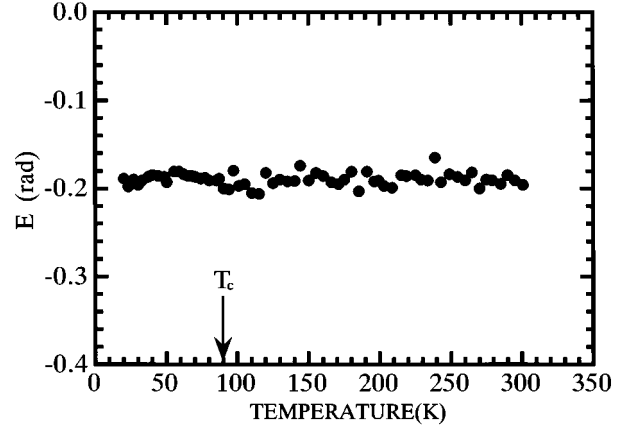
FIG. 5. Temperature dependence of linear dichroism E of BSCCO.

the specimen through the front surface, and the next ones with light passing it through the rear surface by reversing the Cu plate itself. If gyrations observed by the front and rear measurements are designated as G^+ and G^-, the reciprocal gyration is given by $G_r = (1/2)(G^+ + G^-)$, and the nonreciprocal gyration by $G_n = (1/2)(G^+ - G^-)$. We will describe in the following the former experiments in detail, but not the latter, since the results of both experiments were found to be the same. The temperatures of the specimen were changed between 15 and 300 K within a stability of ± 0.02 K at each temperature. An Ar laser with wavelength $\lambda = 488$ nm was used as the light source.

The HAUP experiments were made only when the extinction ratios of the crossed Nicols condition were found to be less than 6×10^{-9}. The temperature dependence of θ_0 is shown in Fig. 3. Within a grid of $\pm 0.1°$ square in the (θ', Υ') coordinate, the intensities of the emergent light were measured at 121 points. By least-squares fittings, values of $I_0 A''(\theta')$, $I_0 B''(\theta')$, and $I_0 C''$ were determined at various temperatures. For examples, relations of $I_0 C''$ vs θ', $I_0 A''$ vs θ'^2, and $I_0 B''$ vs θ' at 300 K are shown in Figs. 4(a), 4(b), and 4(c), respectively. Linear relations hold in each figure, as were the cases for elbaite. E, Δ, and $B''(0)$ could be obtained. Temperature dependence of E is shown in Fig. 5, where E stayed almost constant at $(-1.90 \pm 0.15) \times 10^{-1}$. E was found to be considerable, and this fact indicated that our extended HAUP method was appropriate for the study of this material. Figures 6 and 7 show temperature dependences of Δ and $B''(0)$, respectively.

The next step, which was the most difficult but important part of this study, was derivations of the systematic errors, p, q, and $\delta\Upsilon$. For this aim, the following two equations were available:

$$B''(0) = \frac{2\,\delta\Upsilon\,\sin^2\Delta}{e^E + e^{-E} - 2\,\cos\Delta}$$

$$- \frac{2\,\sin\Delta\{(p-q)\cos\Delta - pe^{-E} + qe^E\}}{e^E + e^{-E} - 2\,\cos\Delta}$$

$$- \frac{2k}{K^2 + 1}\sin\Delta, \tag{43}$$

FIG. 4. $I_0 C''$ vs θ' (a), $I_0 A''$ vs θ'^2 (b), and $I_0 B''$ vs θ' (c) for BSCCO at 300 K.

and
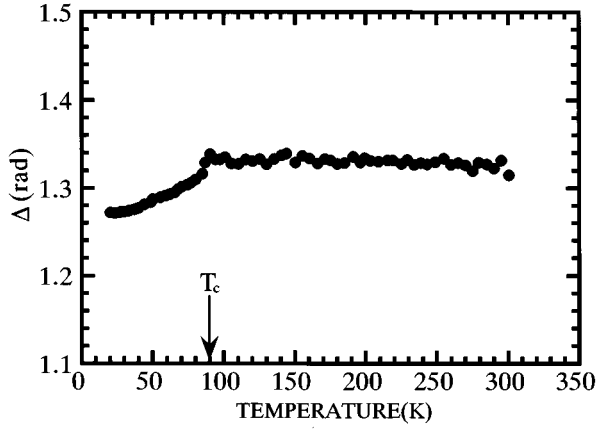
FIG. 6. Temperature dependence of retardation Δ of BSCCO.

$$\theta_0 = \frac{-\sin\Delta}{e^E + e^{-E} - 2\,\cos\Delta}(p+q) - \frac{(e^E - \cos\Delta)}{e^E + e^{-E} - 2\,\cos\Delta}\delta Y$$

$$+ \frac{Kk+k'}{K^2+1} + \alpha. \qquad (44)$$

Here it must be noticed that for θ_0 only the relative values are accurate. Therefore an arbitrary constant α should be added to it as shown in (44). We had already determined $p = -1.5 \times 10^{-4}$ by using a test crystal of $LiNbO_3$.[14] The determinations of $\hat{p}(=p)$, common ellipticity of $LiNbO_3$ and BSCCO systems, have been described in our previous work.[14,18,19] Wavelength dependences of $B''(0)$, E, and Δ were measured at room temperature by using Ar, dyes, and He-Ne lasers. The results are indicated in Figs. 8–10. Then the unknown quantities in (43) became δY, q, and k as more intelligibly expressed below:

$$B''(0) = \frac{2\,\sin^2\Delta}{e^E + e^{-E} - 2\,\cos\Delta}\delta Y - \frac{2\,\sin\Delta(e^E - \cos\Delta)}{e^E + e^{-E} - 2\,\cos\Delta}q$$

$$- \frac{2\,\sin\Delta}{K^2+1}k + \frac{2\,\sin\Delta(e^{-E} - \cos\Delta)}{e^E + e^{-E} - 2\,\cos\Delta}p, \qquad (45)$$

Here we defined a residual $R(\lambda)$ which is functions of δY, q, and k,

$$R(\lambda) = \sum_\lambda \{B''(0,\lambda)^{obs} - B''(0,\lambda)^{cal}\}^2. \qquad (46)$$

We made successive approximations. Assuming first that k was independent of λ, we searched for the optimum values of δY and q, which minimized $R(\lambda)$. They were 7.3×10^{-4}, and 8.1×10^{-4} respectively. By using these values, the wavelength dependence of k was calculated from Fig. 8. The result is shown in Fig. 11 by full circles. It was clear at this stage that k was nearly zero and independent of λ. We repeated the process of determining both errors by using this wavelength dependence of k. The results were $\delta Y = 7.2 \times 10^{-4}$, and $q = 7.9 \times 10^{-4}$, and k dependence was unchanged as shown in Fig. 11 by the open triangles. It was evident that both errors did not change appreciably from the previous ones and the wavelength dependence of k also did not change. In order to confirm that we obtained the correct values, θ_0 values were calculated by using the final values of

the errors and compared them with the observed values in Fig. 12. The agreement was excellent, the separation of both series being caused by α. Thus the systematic errors have been determined as

$$p = -1.5 \times 10^{-4},$$

$$q = 7.9 \times 10^{-4},$$

and

$$\delta Y = 7.2 \times 10^{-4}. \qquad (47)$$

By using these systematic errors, k, G which is g_{33} in the present case, Δn, and Δm were derived from Figs. 5, 6, and 7. the temperatures dependences of these quantities are shown in Figs. 13–16, respectively. As noted before, these results were obtained from the front surface experiments. We repeated the HAUP measurements with the incident light beam propagating to the opposite directions of the specimen. Almost the same results were obtained as for the front surface experiments. Therefore we do not describe them again.

From Fig. 14, an important result was obtained, BSCCO does not produce any signs of Faraday effect in the whole temperature range including T_c, and becomes optically active in the superconducting state. These facts also verify that the approximation conditions (22) of our extended HAUP method were properly fulfilled in the present experiments. Besides, as it can be seen from Fig. 15, the birefringence Δn also manifests a steep temperature change below T_c. The coefficients of thermal changes of g_{33} and Δn are expressed in Figs. 17(a), and 17(b). From the behaviors of these temperature coefficients it can be concluded that BSCCO undergoes a second-order structural phase transformation to an optically active phase at the onset of the superconductivity. In addition, BSCCO exhibits large LD, $\Delta m = -2.2 \times 10^{-2}$, in the present temperature range. It is about three orders of magnitude larger than those of elbaite.

IV. DISCUSSION

As a way for examining the validity of the present data, our results of Δn and Δm were compared with those derived
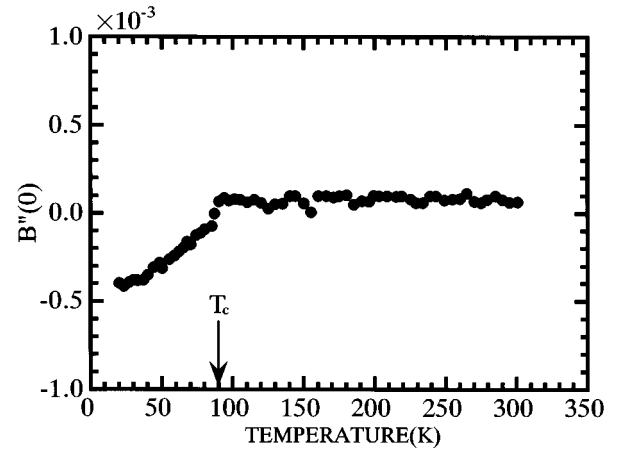
FIG. 7. Temperature dependence of $B''(0)$ of BSCCO.
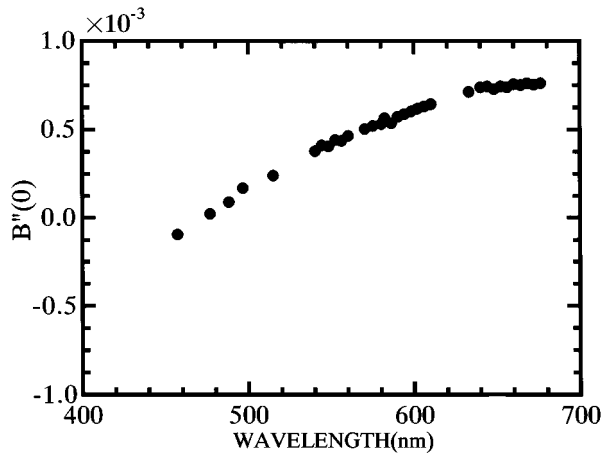
FIG. 8. Wavelength dependence of $B''(0)$ of BSCCO.
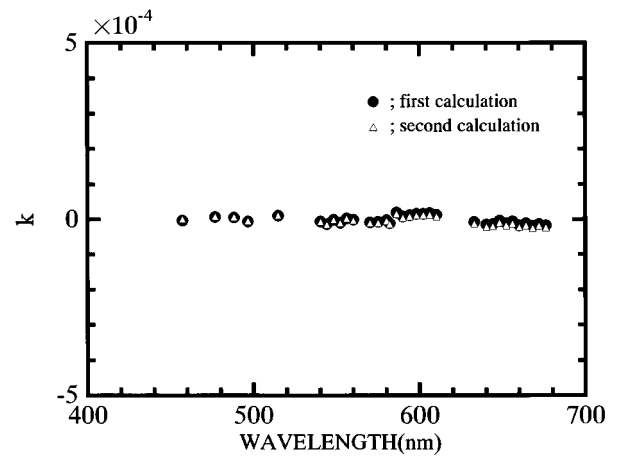
FIG. 11. Wavelength dependences of ellipticity k of BSCCO calculated by successive approximations.
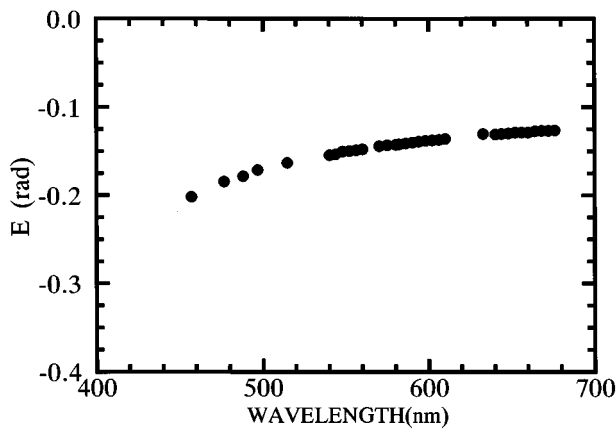
FIG. 9. Wavelength dependence of linear dichroism E of BSCCO.
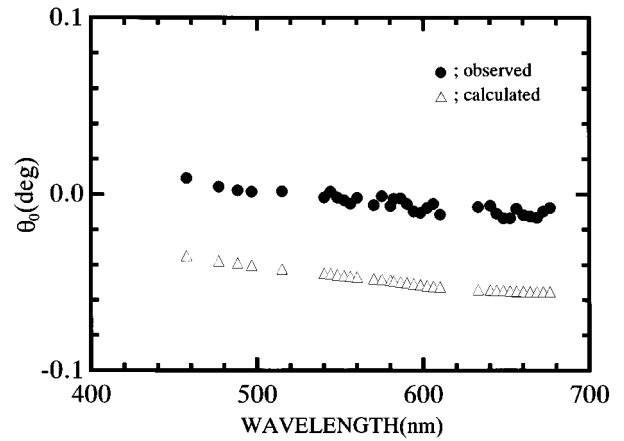
FIG. 12. Wavelength dependences of the observed and calculated θ_0 of BSCCO.
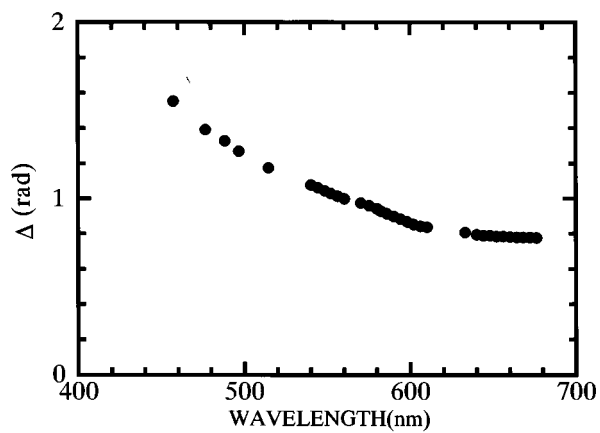
FIG. 10. Wavelength dependence of retardation Δ of BSCCO.
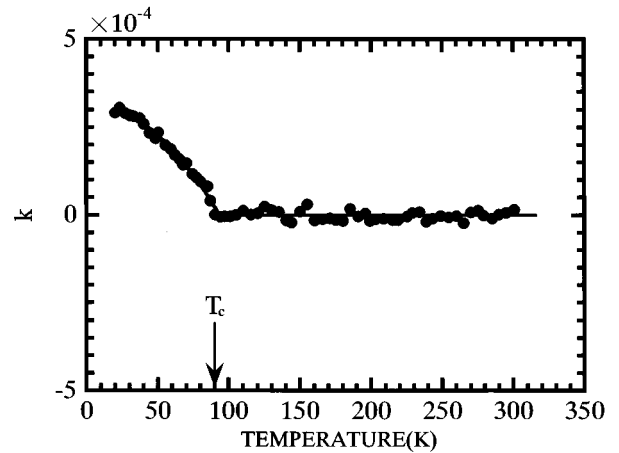
FIG. 13. Temperature dependence of ellipticity k of BSCCO.
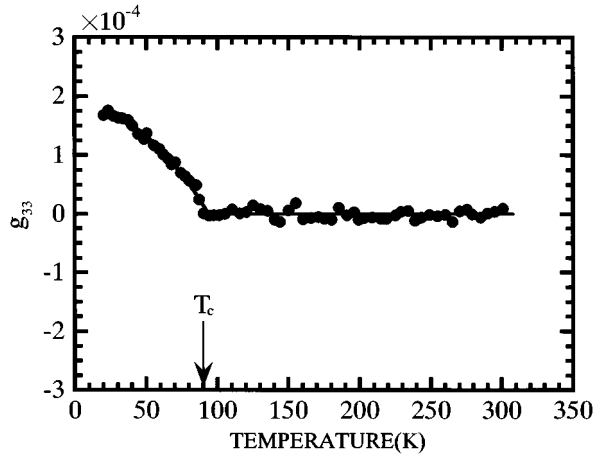
FIG. 14. Temperature dependence of gyration tensor component g_{33} of BSCCO.

from optical reflection measurements by Zibold *et al.*[26] They measured polarized reflectance spectra of this crystal between 0.03 and 6 eV at room temperature. By using the fitting processes of the Lorentz-Drude model and a Kramers-Kronig analysis, they showed anisotropic tensor components of the energy-loss function $Im(-1/\varepsilon)$ and the conductivity function σ along the crystallographic axes as a function of frequency ν of light, where ε and σ are expressed as $\varepsilon = \varepsilon_1 + i\varepsilon_2$ and $\sigma = 2\pi\nu\varepsilon_2\varepsilon_0$. For $\lambda = 488$ nm, these components are given as follows: $Im(-1/\varepsilon^a) = 0.115$ for the a axis, $Im(-1/\varepsilon^b) = 0.085$ for the b axis, and $Im(-1/\varepsilon^c) = 0.062$ for the c axis, and $\sigma^a = 5.6 \times 10^2$, $\sigma^b = 5.4 \times 10^2$, and $\sigma^c = 4.2 \times 10^2$. Then the components of ε along each axis are derived as $\varepsilon_1^a = 3.40$ and $\varepsilon_2^a = 1.64$, $\varepsilon_1^b = 4.01$ and $\varepsilon_2^b = 1.58$, and $\varepsilon_1^c = 4.27$ and $\varepsilon_2^c = 1.23$. As ε_1 and ε_2 are related to n and m by the relations, $\varepsilon_1 = n^2 - m^2$ and $\varepsilon_2 = 2nm$, the refractive indices are derived as

$$n_a = 1.89,$$

$$n_b = 2.04,$$

and
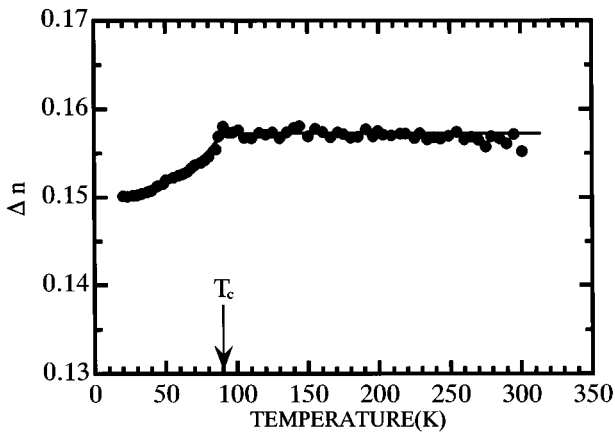
FIG. 15. Temperature dependence of birefringence Δn of BSCCO.
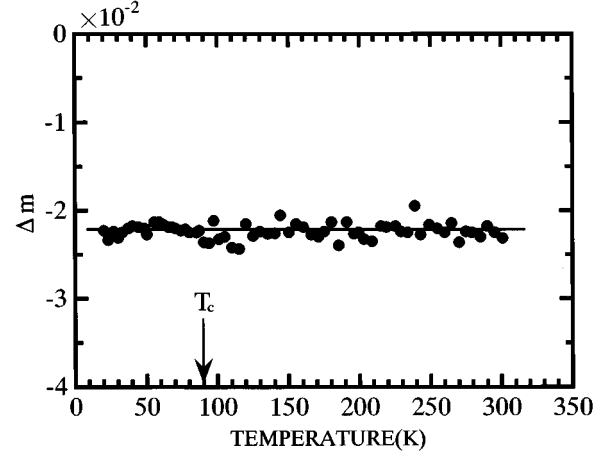
FIG. 16. Temperature dependence of Δm of BSCCO.

$$n_c = 2.09. \tag{48}$$

The sequence of the magnitudes of the refractive indices, say, $n_a < n_b < n_c$, accords with our result derived from the conoscopic observation, and $\Delta n = n_b - n_a = 0.15$ is in good agreement with our result of 0.157. On the other hand, m values are given as

$$m_a = 0.43,$$

$$m_b = 0.39,$$
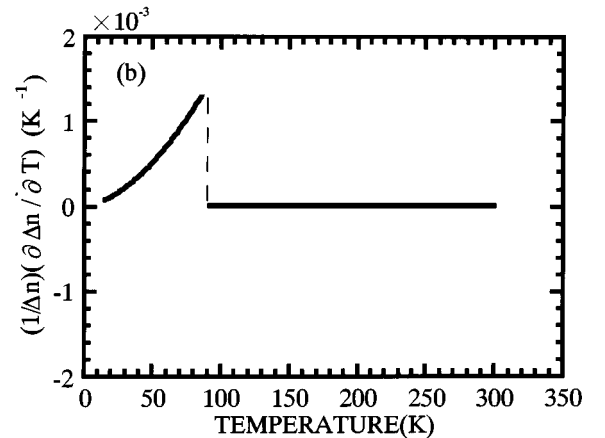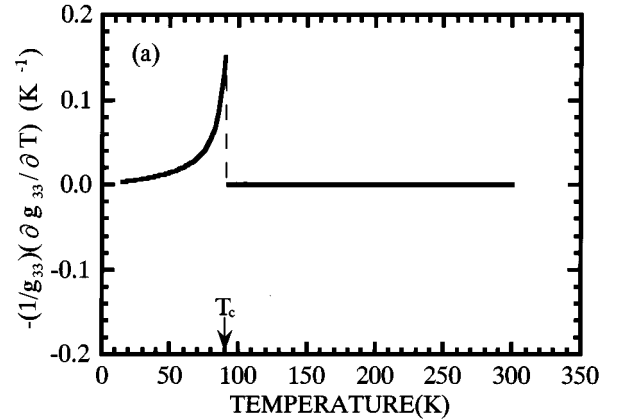
FIG. 17. Temperature dependences of thermal coefficients of (a) g_{33} and (b) Δn of BSCCO.

and

$$m_c = 0.29. \tag{49}$$

$\Delta m = m_b - m_a = -0.04$ is not largely different from our result of -0.022. Thus the work by Zibold *et al.* supports a part of our data. Bozovic[27] determined average values of the dielectric constants, which agreed with values calculated from the data of Zibold.[26]

Temperature dependences of Δn shown in Fig. 15 and of Δm in Fig. 16 may appear contradictory at a glance from the Kramers-Kronig relation. The standard deviations of Δn and Δm are in the same order of magnitude, say, 5×10^{-5} and 9×10^{-5}, respectively. However the values of Δn are approximately one order of magnitude larger than Δm. Then it follows that the change of the same order of magnitude of Δm as that of Δn (about 4% in maximum) cannot be detected in Fig. 16.

We took care of the effect of the reflectance on the front and back surfaces on CD. Specimens with different thickness, say, 0.79, 0.66 (the present specimen), 0.47, and 0.35 μm were used for the test. They provided us with almost the same results.

It is important to note that the present experiments were made on a single domain crystal. This is ensured by the fact that a beam of small size was incident upon a very thin specimen which produced typical conoscopic figures. The specimen produced gyration below T_c but no signs of non-

reciprocal effect of it. Therefore the present results do not seem to agree with the evidence reported by Lyons and co-workers[4–6] but support the conclusions of Lawrence, Szöke, and Laughlin.[28] However, it must be noted that the results of Lyons *et al.* were derived from reflection measurements. Above all, considering the possibility of an antiferromagnetic (AFM) model,[29–32] it might be premature to draw a decisive conclusion on the violation of time-reversal symmetry in the superconducting state, Canright and Rojo[30,31] showing explicitly that the reciprocal gyration also occurs for the AFM model. It has been clearly revealed that the symmetry of parity is lost in the superconducting phase. Spielman and co-workers[7–9] used a Sagnac interferometer which could detect only nonreciprocal effects but reject any reciprocal ones. Therefore their results are not inconsistent with our results.

Closing the paper we think it of particular importance to stress that BSCCO undergoes a structural phase transition together with the onset of superconductivity. This fact should be taken into account for the elucidations of the mechanism of high-temperature superconductivity.

APPENDIX: EXPRESSIONS OF THE COEFFICIENTS H_{ij} IN (11)

Each coefficient H_{ij} in (11) is expressed as follows:

$$H_{11} = \frac{(\cosh 2xd - \cos 2yd)\{\omega^2 + \delta^2 + 2(p-q)(p_0\delta - g_0\omega)\}}{2(x^2 + y^2)} + \frac{(\cosh 2xd - \cos 2yd)\{(p-q)^2(p_0^2 + g_0^2 - \omega^2 - \delta^2)\}}{2(x^2 + y^2)}$$

$$+ \frac{\sinh 2xd\{(p+q)(\omega y - \delta x) - (p^2 - q^2)(p_0 x + g_0 y)\}}{x^2 + y^2} - \frac{\sin 2yd\{(p+q)(\omega x + \delta y) + (p^2 - q^2)(p_0 y - g_0 x)\}}{x^2 + y^2}$$

$$+ \frac{(\cosh 2xd + \cos 2yd)(p+q)^2}{2},$$

$$H_{12} = \frac{2(p_0\omega + g_0\delta)(-\cosh 2xd + \cos 2yd)}{(x^2 + y^2)} + \frac{2(p+q)\{(-p_0 y + g_0 x)\sinh 2xd + (p_0 x + g_0 y)\sin 2yd\}}{(x^2 + y^2)},$$

$$H_{13} = \frac{2(p_0^2 + g_0^2)(\cosh 2xd - \cos 2yd)}{x^2 + y^2},$$

$$H_{21} = \frac{(p_0\omega + g_0\delta)(-\cosh 2xd + \cos 2yd)}{x^2 + y^2} + \frac{\sinh 2xd\{2p(-p_0 y + g_0 x) - (\omega x + \delta y)\}}{x^2 + y^2} + \frac{\sin 2yd\{2p(p_0 x + g_0 y) - \omega y + \delta x\}}{x^2 + y^2},$$

$$H_{22} = \frac{2(p_0^2 + g_0^2)(\cosh 2xd - \cos 2yd)}{x^2 + y^2} + \frac{2\{(p_0 x + g_0 y)\sinh 2xd + (p_0 y - g_0 x)\sin 2yd\}}{x^2 + y^2},$$

and

$$H_{31} = \frac{(p_0^2 + g_0^2 + \omega^2 - \delta^2)(\cosh 2xd - \cos 2yd)}{2(x^2 + y^2)} + \frac{(\cosh 2xd + \cos 2yd)}{2} + \frac{\sinh 2xd(p_0 x + g_0 y)}{x^2 + y^2} + \frac{\sin 2yd(p_0 y - g_0 x)}{x^2 + y^2}.$$

[1] R. B. Laughlin, Science **242**, 525 (1988).

[2] X. G. Wen and A. Zee, Phys. Rev. Lett. **62**, 2873 (1989).

[3] B. I. Halperin, J. March-Russel, and F. Wilczek, Phys. Rev. B **40**, 8726 (1989).

[4] K. B. Lyons, J. Kwo, J. F. Dillon, Jr., G. P. Espinosa, M. McGlashan-Powell, A. P. Ramirez, and L. F. Schneemeyer, Phys. Rev. Lett. **64**, 2949 (1990).

[5] K. B. Lyons, J. F. Dillon, Jr., E. S. Hellman, E. H. Hartford, and M. McGlashan-Powell, Phys. Rev. B **43**, 11 408 (1991).

[6] K. B. Lyons, J. F. Dillon, Jr., S. J. Duclos, C. B. Eom, H. L. Kao, J. Kwo, J. M. Phillips, and M. P. Siegal, Phys. Rev. B **47**, 8195 (1993).

[7] S. Spielman, K. Fesler, C. B. Eom, T. H. Geballe, M. M. Fejer, and A. Kapitulnik, Phys. Rev. Lett. **65**, 123 (1990).

[8] S. Spielman, J. S. Dodge, K. Fesler, L. W. Lombardo, M. M. Fejer, T. H. Geballe, and A. Kapitulnik, Phys. Rev. B **45**, 3149 (1992).

[9] S. Spielman, J. S. Dodge, L. W. Lombardo, C. B. Eom, M. M. Fejer, T. H. Geballe, and A. Kapitulnik, Phys. Rev. Lett. **68**, 3472 (1992).

[10] H. J. Weber, D. Weitbecht, D. Brach, A. L. Shelankov, H. Keiter, W. Weber, Th. Wolf, J. Geerk, G. Linker, G. Roth, P. C. Splittgerber-Hünnekes, and G. Güntherodt, Solid State Commun. **76**, 511 (1990).

[11] For instance, J. Kobayashi, K. Saito, N. Takahashi, and I. Kamiya, Phys. Rev. B **48**, 10 038 (1993); and J. Kobayashi, T. Asahi, M. Ichiki, K. Saito, T. Shimasaki, H. Yoshii, Y. Itagaki, and H. Ikawa, *ibid.* **51**, 763 (1995).

[12] J. Kobayashi and Y. Uesu, J. Appl. Crystallogr. **16**, 204 (1983).

[13] J. Kobayashi, H. Kumomi, and K. Saito, J. Appl. Crystallogr. **19**, 377 (1986).

[14] J. Kobayashi, T. Asahi, S. Takahashi, and A. M. Glazer, J. Appl. Crystallogr. **21**, 479 (1988).

[15] J. R. L. Moxon and A. R. Renshaw, J. Phys. C **2**, 6807 (1990).

[16] E. Dijkstra, H. Meekes, and M. Kremers, J. Phys. D **24**, 1861 (1991).

[17] R. C. Jones, J. Opt. Soc. Am. **38**, 671 (1948).

[18] J. Kobayashi, K. Saito, N. Takahashi, and I. Kamiya, Phys. Rev. B **49**, 6539 (1994).

[19] J. Kobayashi, K. Saito, N. Takahashi, I. Kamiya, and H. Utsumi, Phys. Rev. B **50**, 2766 (1994).

[20] J. R. L. Moxon, A. R. Renshaw, and I. J. Tebbutt, J. Phys. D **2**, 1187 (1991).

[21] M. J. Buerger and W. Parish, Amer. Min. **22**, 113 (1937).

[22] T. Ito and R. Sadanaga, Acta Crystallogr. **4**, 385 (1951).

[23] R. W. T. Wilkins, E. F. Farrell, and C. S. Naiman, J. Phys. Chem. Solids **30**, 43 (1969).

[24] A. Yariv and P. Yeh, *Optical Waves in Crystals* (Wiley, New York, 1984), p. 85.

[25] Y. Gao, P. Lee, P. Coppens, M. A. Subramanian, and A. W. Sleight, Science **241**, 954 (1988).

[26] A. Zibold, M. Dürrler, A. Gaymann, H. P. Geserich, N. Nücker, V. M. Burlakov, and P. Müller, Physica C **193**, 171 (1992).

[27] I. Bozovic, Phys. Rev. B **42**, 1969 (1990).

[28] Taylor W. Lawrence, A. Szöke, and R. B. Laughlin, Phys. Rev. Lett. **69**, 1439 (1992).

[29] I. E. Dzyaloshinskii, Phys. Lett. A **155**, 62 (1991).

[30] G. S. Canright and A. G. Rojo, Phys. Rev. Lett. **68**, 1601 (1992).

[31] G. S. Canright and A. G. Rojo, Phys. Rev. B **46**, 14 078 (1992).

[32] G. S. Canright and M. D. Johnson, J. Phys. A **27**, 3579 (1994).